Copyright © 2008 by the Genetics Society of America
DOI: 10.1534/genetics.108.090654

Mutants Defective in Rad1-Rad10-Slx4 Exhibit a Unique Pattern of Viability During Mating-Type Switching in *Saccharomyces cerevisiae*

Amy M. Lyndaker, Tamara Goldfarb[1] and Eric Alani[2]

Department of Molecular Biology and Genetics, Cornell University, Ithaca, New York 14853-2703

Manuscript received April 24, 2008
Accepted for publication May 22, 2008

ABSTRACT

Efficient repair of DNA double-strand breaks (DSBs) requires the coordination of checkpoint signaling and enzymatic repair functions. To study these processes during gene conversion at a single chromosomal break, we monitored mating-type switching in *Saccharomyces cerevisiae* strains defective in the Rad1-Rad10-Slx4 complex. Rad1-Rad10 is a structure-specific endonuclease that removes 3′ nonhomologous single-stranded ends that are generated during many recombination events. Slx4 is a known target of the DNA damage response that forms a complex with Rad1-Rad10 and is critical for 3′-end processing during repair of DSBs by single-strand annealing. We found that mutants lacking an intact Rad1-Rad10-Slx4 complex displayed *RAD9*- and *MAD2*-dependent cell cycle delays and decreased viability during mating-type switching. In particular, these mutants exhibited a unique pattern of dead and switched daughter cells arising from the same DSB-containing cell. Furthermore, we observed that mutations in post-replicative lesion bypass factors (*mms2*Δ, *mph1*Δ) resulted in decreased viability during mating-type switching and conferred shorter cell cycle delays in *rad1*Δ mutants. We conclude that Rad1-Rad10-Slx4 promotes efficient repair during gene conversion events involving a single 3′ nonhomologous tail and propose that the *rad1*Δ and *slx4*Δ mutant phenotypes result from inefficient repair of a lesion at the *MAT* locus that is bypassed by replication-mediated repair.

IN the baker's yeast *Saccharomyces cerevisiae*, spontaneous and induced DNA double-strand breaks (DSBs) are primarily repaired by homologous recombination (reviewed in Pâques and Haber 1999). In the initial steps of repair, DSBs are acted upon by a 5′–3′ exonuclease activity to yield two 3′ single-stranded ends. These ends interact with RPA, Rad51, Rad52, Rad54, Rad55, and Rad57 to allow strand invasion into a homologous double-stranded donor sequence. DNA synthesis initiating from the 3′ invading end results in copying of DNA sequence from the donor locus, and recombination is completed either by resolution of a Holliday junction intermediate or by synthesis-dependent strand annealing (SDSA). Homologous recombination can also occur by nonconservative mechanisms including single-strand annealing (SSA) and break-induced replication (BIR). During SSA, a DSB located between repeated sequences is processed by 5′–3′ exonuclease activity and the 3′ single-stranded ends anneal at homologous sequences, resulting in deletion of the intervening sequence. In BIR, strand invasion of one 3′-end into a homologous sequence is followed by replication that continues along the chromosome arm (reviewed in Pâques and Haber 1999).

Mating-type switching in *S. cerevisiae* is a unidirectional gene conversion event in which a DSB created at the *MAT* locus is repaired using one of two silent mating-type cassettes, *HMR***a** or *HML*α (reviewed in Haber 1998). This programmed recombination event is initiated by HO endonuclease cleavage within *MAT*, and donor preference is such that cells preferentially repair the DSB using the donor sequence of the opposite mating type (Wu and Haber 1995, 1996; Wu *et al.* 1997; Haber 1998). Crossovers, which would lead to intrachromosomal deletions, are rarely associated with mating-type switching (Klar and Strathern 1984), and mating-type switching is thought to occur by a SDSA mechanism (McGill *et al.* 1989; Haber 1998; Pâques and Haber 1999; Ira *et al.* 2006).

The HO cleavage site at the *MAT* locus is located at the junction between homologous and nonhomologous sequence with respect to the donor cassette. Strand invasion is thought to be initiated by the 3′ tail that is homologous to the donor sequence, leaving the second 3′-end as a nonhomologous tail following annealing of the repaired invading strand (Figure 1A). Thus, a single 3′ nonhomologous tail must be removed to complete repair. Previous genetic studies have shown that 3′ nonhomologous tail removal depends on the activity of the Rad1-Rad10 endonuclease, as well as the Msh2-Msh3 DNA mismatch recognition complex (Fishman-Lobell

[1]*Present address:* Center for Cancer Research, National Cancer Institute, Bethesda, MD 20892-4255.

[2]*Corresponding author:* Department of Molecular Biology and Genetics, Cornell University, 459 Biotechnology Bldg., Ithaca, NY 14853-2703. E-mail: eea3@cornell.edu

and Haber 1992; Ivanov and Haber 1995; Kirkpatrick and Petes 1997; Saparbaev *et al.* 1996; Sugawara *et al.* 1997).

Rad1-Rad10 is a structure-specific endonuclease that cleaves DNA at the junction of double-stranded and 3′ single-stranded DNA (ssDNA) and has been characterized in its role during nucleotide excision repair (NER) as well as in the removal of 3′ nonhomologous tails and blocked 3′ termini, including Top1-associated DNA (Sung *et al.* 1993; Bardwell *et al.* 1994; Vance and Wilson 2002; Guzder *et al.* 2004). The importance of Rad1-Rad10 for its non-NER DNA processing functions is highlighted by the fact that mice lacking the mammalian homolog of Rad1-Rad10, ERCC1-XPF, exhibit features of premature aging, including a very reduced life span (20–38 days), severe runting, and abnormalities of the liver, skin, kidney, and spleen, while mice lacking other NER factors develop normally and have a normal life span (McWhir *et al.* 1993; Weeda *et al.* 1997).

In plasmid-based studies, both Rad1-Rad10 and Msh2-Msh3 are required for recombinational repair when two 3′ nonhomologous tails are present (Sugawara *et al.* 1997; Colaiácovo *et al.* 1999). Repair events involving only one nonhomologous end are also hypothesized to require Rad1-Rad10 and Msh2-Msh3, although a second, less efficient pathway involving the 3′–5′ proofreading activity of DNA polymerase δ has been shown to remove 3′ ssDNA <30 nucleotides long (Pâques and Haber 1997; Colaiácovo *et al.* 1999). The Haber lab previously reported that mating-type switching in G_1-arrested cells is significantly less efficient in *rad1*Δ mutants, but stated no further defects (Holmes and Haber 1999b).

Rad1-Rad10 and Msh2-Msh3 are also required during SSA, which involves two nonhomologous tails. The requirement for Msh2-Msh3 depends on the length of the annealed region; annealed regions >1 kb in length are repaired independently of Msh2-Msh3. Thus, Msh2-Msh3 is thought act by binding and stabilizing the double-strand/single-strand junctions to promote Rad1-Rad10-dependent cleavage of 3′-ends (Sugawara *et al.* 1997; Pâques and Haber 1999). Consistent with this, *in vitro* biochemical studies have shown that purified Msh2-Msh3 binds specifically to double-strand/single-strand junctions and opens up the junction, possibly providing a more suitable substrate for Rad1-Rad10 cleavage (Surtees and Alani 2006). Recent work from Flott *et al.* (2007) has also implicated the Slx4 protein in Rad1-Rad10-dependent 3′ nonhomologous tail removal. The authors found that Slx4 forms a complex with Rad1-Rad10 that is mutually exclusive of the interaction with its endonuclease partner, Slx1. Slx4 was found to be required for Rad1-dependent DSB repair by single-strand annealing, presumably at the 3′ nonhomologous tail removal step (Flott *et al.* 2007).

A single unrepaired DSB is sufficient to trigger G_2/M cell cycle arrest in *S. cerevisiae* (Sandell and Zakian 1993). Arrest at the G_2/M transition can be elicited by the DNA damage or spindle checkpoints. While cell cycle checkpoints are not normally activated during mating-type switching, the DNA damage response is activated in strains lacking both donor sequences, which are thus unable to repair the DSB by gene conversion (Pellicioli *et al.* 1999, 2001; Lee *et al.* 2003). Activation of the DNA damage checkpoint has also been shown to occur during DSB repair at *MAT* when the donor locus is on a separate chromosome, most likely because the repair process takes longer to occur (Vaze *et al.* 2002). A role for the spindle checkpoint during mating-type switching has not been reported.

In this study, we used a variety of techniques to examine the importance of the Rad1-Rad10-Slx4 complex in 3′ nonhomologous tail removal during mating-type switching. We show that mutants defective in the Rad1-Rad10-Slx4 complex exhibited a *RAD9*-dependent, partially *MAD2*-dependent cell cycle arrest and decreased cell survival during mating-type switching. A third of *rad1*Δ and *slx4*Δ cells induced for mating-type switching showed a unique viability profile during pedigree analysis, with one switched and one dead daughter cell arising from the same DSB-induced cell. We hypothesize that this phenotype arises from replication bypass of an inefficiently repaired DNA lesion at *MAT*. This work indicates that the Rad1-Rad10-Slx4 complex promotes the efficient repair of DSBs involving a single 3′ nonhomologous tail intermediate.

MATERIALS AND METHODS

Strains and plasmids: All strains used in this study are shown in Table 1. Parental strains EAY745 (*MAT***a** to *MAT*α), EAY 744 (*MAT***a** to *MAT***a**), and EAY742 (*donorless*) were created by single-step gene replacement with *Sph*I- and *Pvu*II-digested pEAI118 to integrate *MSH2-HA*$_4$*::LEU2* at the endogenous *MSH2* locus in JKM161, JKM160, or JKM139, respectively, and were kindly provided by J. Haber. Insertion of the HA_4 epitope into Msh2 did not disrupt gene function (Goldfarb and Alani 2004). All strains contain an HO endonuclease gene under control of the galactose-inducible *GAL10* promoter to allow for inducible mating-type switching. To create the parental strain EAY1042 used in the double nonhomology experiments (Figure 1; supplemental Figure 1; Table 1), EAY745 was transformed with a PCR-generated fragment containing 57 bp of **Y**a sequence proximal to the *MAT* HO cut site, 1428 bp of *KANMX* sequence, and 52 bp of sequence distal to the HO cut site. Integration of the *KANMX*-containing fragment (*MAT***a**::*KANMX4*) was confirmed by both PCR and Southern blot analysis. Yeast were transformed with the appropriate DNA fragments using the lithium acetate method (Gietz and Schiestl 1991), and integrations were confirmed by PCR followed by phenotype testing.

Media and culture conditions: For time-course experiments, dilutions of stationary phase cultures were made in yeast–peptone (Difco) medium, pH 6.8, containing 2% (w/v) lactate and grown at 30° until mid-log phase (1–2 × 10^7 cells/ml). Cultures were induced with galactose (U.S. Biological) to 2% (w/v) final concentration and samples were collected at relevant time points. HO expression was suppressed after

TABLE 1

Strains used in this study

Name	Genotype	Strain notes and deletion constructs
		*MAT***a** to *MAT*α
EAY745	Wild type	Derived from JKM161 (Δ*ho, HML*α, *MAT***a**, Δ*hmr::ADE1, ade1-100, leu2-3,112, lys5, trp1::hisG, ura3-52, ade3::GAL10::HO*)
EAY853	*rad1*Δ	pWS1510 (*rad1*Δ*::URA3*; E. Friedberg)
EAY969	*msh2*Δ	pEAI99 (*msh2*Δ*::TRP1*; this lab)
EAY854	*msh3*Δ	pEAI88 (*msh3*Δ*::hisG-URA3-hisG*; this lab)
EAY2087	*slx4*Δ	*slx4*Δ*::KANMX*
EAY1788	*pol3-01*	YIpAM26 (*pol3-01::URA3*; from A. Sugino)
EAY1332	*mus81*Δ	*mus81*Δ*::KANMX*
EAY1730	*rad9*Δ	*rad9*Δ*::KANMX*
EAY1968	*mad2*Δ	*mad2*Δ*::KANMX*
EAY1562	*mms2*Δ	*mms2*Δ*::KANMX*
EAY1778	*mph1*Δ	*mph1*Δ*::KANMX*
EAY2125	*rad1*Δ*rad10*Δ	*rad10*Δ*::KANMX*; see above
EAY2090	*rad1*Δ*slx4*Δ	See above
EAY1803	*rad1*Δ *pol3-01*	See above
EAY797	*rad1*Δ*mus81*Δ	See above
EAY1726	*rad1*Δ*rad9*Δ	See above
EAY1973	*rad1*Δ *mad2*Δ	See above
EAY1725	*rad1*Δ*mms2*Δ	See above
EAY1776	*rad1*Δ *mph1*Δ	See above
		*MAT***a** to *MAT***a**
EAY744	Wild type	Derived from JKM160 (Δ*ho,* Δ*hml::ADE1, MAT***a**, *HMR***a**, *ade1-100, leu2-3,112, lys5, trp1::hisG, ura3-52, ade3::GAL10::HO*)
EAY1356	*rad1*Δ	pWS1510 (*rad1*Δ*::URA3*; E. Friedberg)
EAY2084	*slx4*Δ	*slx4*Δ*::KANMX*
		*MAT***a***::KANMX* to *MAT*α
EAY1042	Wild type	Derived from JKM161; see MATERIALS AND METHODS
EAY1115	*rad1*Δ	pWS1510 (*rad1*Δ*::URA3*; E. Friedberg)
EAY1040	*msh2*Δ	pEAI99 (*msh2*Δ*::TRP1*)
EAY1118	*msh3*Δ	pEAI88 (*msh3*Δ*::hisG-URA3-hisG*)
EAY1407	*rad51*Δ	pJH683 (*rad51*Δ*::URA3*; from J. Haber)
		donorless
EAY742	Wild type	Derived from JKM139 (Δ*ho,* Δ*hml::ADE1, MAT***a**, Δ*hmr::ADE1, ade1-100, leu2-3,112, lys5, trp1::hisG, ura3-52, ade3::GAL10::HO*)

All strains used in this study are derived from JKM161, JKM160, and JKM139, kindly provided by J. Haber. Gene disruptions and mutant alleles were made by transforming *S. cerevisiae* strains with restriction-digested plasmids for *rad1*Δ, *msh2*Δ, *msh3*Δ, *rad51*Δ, and *pol3-01* as listed above. All other disruptions were made by integrative transformation of PCR products generated by amplification of *KANMX* sequences from either plasmid pFA6-KanMX4 (WACH *et al.* 1994) or genomic DNA from the *Saccharomyces* Genome Deletion Project knockout strains (http://www-sequence.stanford.edu/group/yeast_deletion_project/deletions3.html). See MATERIALS AND METHODS for details.

30 min by the addition of glucose (U.S. Biological) to 2% (w/v) final concentration. To maintain a consistent number of cells at each time point throughout the time course, individual samples were diluted to the same cell density as the time zero sample.

Cell survival assays: Asynchronous cultures were grown to mid-log phase and induced with galactose for 30 min. Uninduced controls were diluted similarly with water. Both induced and uninduced cultures were diluted 2500-fold and plated in triplicate on YPD plates immediately following the addition of glucose to the media. After growth for 3 days at 30°, the percentage survival was calculated as the number of colonies arising from induced relative to uninduced cultures. At least four independent cultures were used for each strain (Table 2). Results are shown as the mean ± SEM and were statistically analyzed using an unpaired two-tailed Student's *t*-test (http://www.physics.csbsju.edu/stats/t-test_bulk_form.html; see RESULTS).

Mating-type switching assay: To determine mating types, individual colonies from cell survival assays (20–40/replicate) were crossed with *arg4 MAT***a** and *MAT*α tester strains (EAY759 and EAY760; from N. Sugawara, Haber laboratory) and replica plated onto synthetic complete plates (ROSE *et al.* 1990) lacking both arginine and lysine to select for diploids. The percentage of switched cells was determined for each cell survival experiment and is shown in Table 2 as the mean ± SEM.

Southern blot analysis: Chromosomal DNA was isolated during time-course experiments as described (Holmes and Haber 1999a; Goldfarb and Alani 2004) following a 30-min galactose induction. DNA was then digested with *Sty*I (New England Biolabs) for single nonhomology strains or with *Ava*II, *Ban*I, and *Blp*I (New England Biolabs) for double nonhomology strains and electrophoresed on 1% TAE–agarose gels with 1× TAE buffer. Southern blot transfer and hybridizations were performed essentially as described by the manufacturer (Amersham) using the Church and Gilbert method (1984).

All probes used for Southern blot analysis were amplified by PCR using EAY745 yeast genomic DNA and ^{32}P-labeled using the NEBlot kit (New England Biolabs) according to the manufacturer's description. To probe *MAT*-specific bands, we radiolabeled a 638-bp PCR product beginning 67 bp downstream of the *MAT Z2* region using pJH364 forward and reverse primers (5′-ACGAATTGGCTATACGGGAC and 5′-GTCCAATCTGTGCACAATGAAG, respectively, from the Haber lab). Efficient DSB formation was detected 30 min after galactose induction by Southern blot analysis (Figure 2). To visualize mating-type switching in double nonhomology strains, probes were produced from a 277-bp PCR product amplified using primers AO585 (5′-CTTAGCATCATTCTT TGTTCTTAT) and AO586 (5′-CAAGAAGGCGAATAAGATA AAGA). Loading control probes for blots of the double nonhomology strains were created by amplifying a 235-bp PCR product with primers AO583 (5′-CTCGTATTGGAGAAA TAAGTTTTCGT) and AO584 (5′-GGTAGAGTCTTATTGG CAAGATAG) (supplemental Figure 1). **Ya**-specific probes (supplemental Figure 2) were created by labeling a 539-bp PCR fragment made using primers AO1425 (5′-GGACAACAT GGATGATATTTGTAGTATGGCGG) and AO1049 (5′-CTG TTGCGGAAAGCTGAAAC), both located within **Ya**. Blots were visualized using the Phosphor Imaging system and quantified using the ImageQuant program (Molecular Dynamics). Quantification of repair efficiency in Figure 2C was done as described previously (Wang *et al.* 2004), with product bands set relative to the first HO cut band and normalized relative to the *MAT* distal band in each lane. **Ya** loss was quantified by setting the **Ya** proximal band in each lane relative to the value at $t = 0$ (supplemental Figure 2).

Chromatin immunoprecipitation: Samples from time-course experiments were chromatin immunoprecipitated as described previously (Goldfarb and Alani 2004). Msh2-HA$_4$ was immunoprecipitated from yeast cell extracts using the 12CA5 monoclonal antibody, and expression of Msh2p-HA$_4$ was confirmed by Western blot (Goldfarb and Alani 2004, 2005). All strains used in the chromatin immunoprecipitation (ChIP) experiments contain a deletion of the *HMR***a** donor so that the *MAT***a** locus could be specifically amplified by PCR. PCR reactions, electrophoresis conditions, and quantification were similar to those described in Evans *et al.* (2000), but with different primer sets. To detect sequences proximal to the DSB, a 267-bp fragment containing the **Ya** sequence was amplified from immunoprecipitated and input chromosomal DNA using AO1048 (5′-TCACCCCAAGCACGGGCATT) and AO1049 (5′-CTGTTGCGGAAAGCTGAAAC), which are adjacent to the HO recognition site (Figure 3). Samples were run on 1.5% TAE–agarose gels and bands were quantified relative to the maximal signal using Scion Image (Scion). Since the input signal decreases during mating-type switching as the **Ya** sequence is removed, the data are presented as the amount of chromatin-immunoprecipitated **Ya** PCR product detected after HO induction relative to that at $t = 0$. A 163-bp *CRY1* control band was also amplified from the chromosomal input DNA using primers AO1106 (5′-CGCCAGAGTTACTGGTGG TATGAAGG) and AO1107 (5′-GGAGTCTTGGTTCTAGTAC CACCGG). The PCR signal was quantified within the linear range of detection, and ChIP was specific to both the epitope tag and formaldehyde crosslinking (Goldfarb and Alani 2004).

FACS analysis: Cells were collected at various times after HO induction as described above. Aliquots of cells were pelleted at the relevant time points, fixed in 70% ethanol, and stored at 4° for up to 7 days. Cell samples were resuspended in 50 mm NaCitrate, pH 7.4, sonicated briefly, and treated for 1 hr with RNase A at 37°, followed by a 1-hr treatment with Proteinase K at 37°. DNA was stained with 1 nm final concentration of Sytox Green (Invitrogen), and samples were analyzed at the Cornell University Biomedical Sciences Flow Cytometry Core Laboratory (Ithaca, NY). Percentage of cells in G_1, S, or G_2/M phases was determined by gating according to 1n and 2*1n DNA content. A representative FACS profile for wild-type cells at $t = 0$ is shown in Figure 4B, with vertical gates for G_1, S, and G_2/M phases. Values shown in Figure 4A reflect the mean of three or more samples per time point ± SEM.

Pedigree analysis: Cells were induced for HO cleavage at *MAT* as described above. Following addition of glucose to the medium at $t = 0.5$ hr, 15 μl of culture was dropped down the center of a YPD plate and single, unbudded cells were separated at 1-cm intervals under the light microscope using a microdissection needle. Cells were visualized beginning at $t = 0.5$ hr, incubated at 30° between manipulations, and monitored every 20–30 min until daughter cells were able to be separated from each other ($t = \sim$4–10 hr). Cells that did not complete cell division within 10 hr were not scored. The length of time required for completion of cell division is reported in Table 4 as the mean of all cells in each category ± SEM. Plates were incubated for 3 days at 30°, and colonies were tested for mating type as described above. Cells were categorized by viability and mating type as shown in Table 3. Pairs of daughter cells scored as both unswitched were not included because we cannot rule out the failure to form a DSB in these cells. The number of cells present in dead cell clusters was also recorded and is visualized in supplemental Figure 3B. Photographs of representative cells (supplemental Figure 3) were taken under the light microscope using a Fuji FinePix S5000 digital camera.

RESULTS

Decreased mating-type switching in the absence of the Rad1-Rad10-Slx4 complex: Rad1-Rad10 and Msh2-Msh3 are proposed to act during mating-type switching in steps involving the removal of a single 3′ nonhomologous tail on the non-invading strand as depicted in Figure 1 (Holmes and Haber 1999b; Pâques and Haber 1999). Previous work examining the role of Rad1-Rad10 during gene conversion primarily utilized plasmid-based assays in which DNA sequence on one or both sides of a DSB site contained nonhomologous sequence with respect to a donor sequence, also present on the plasmid (Sugawara *et al.* 1997; Colaiácovo *et al.* 1999). To examine the coordination of repair and checkpoint signaling factors during gene conversion on the chromosome, we analyzed roles for Rad1-Rad10-Slx4 and Msh2-Msh3 in mating-type switching in *S. cerevisiae*, which is hypothesized to involve removal of a single 3′ nonhomologous tail following the annealing step of SDSA (Figure 1A; Haber 1998; Pâques and Haber 1999; Ira *et al.* 2006).

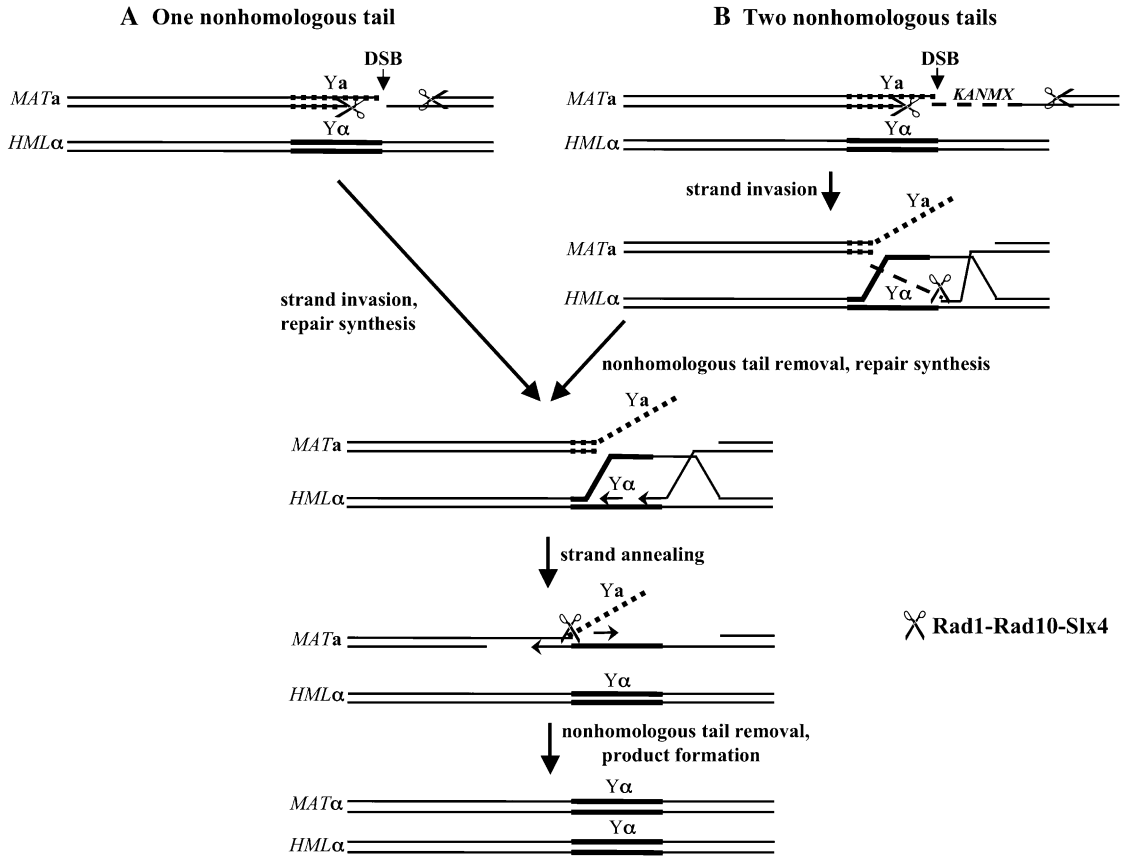

FIGURE 1.—Synthesis-dependent strand annealing model for mating-type switching in *S. cerevisiae* (adapted from PÂQUES and HABER 1999). (A) Only the *MAT***a** and *HML*α loci are shown. Mating-type switching is initiated by a DSB formed by HO endonuclease at the *MAT***a** locus near the Y/Z1 junction. This is followed by 5′–3′ resection to create 3′ single-stranded ends, and the 3′-end with homology to the *HML*α donor sequence initiates strand invasion and primes DNA synthesis off of the donor template. Strand displacement from the donor sequence followed by annealing onto the broken chromosome results in the formation of a 3′ single-stranded nonhomologous tail that must be excised prior to the subsequent DNA synthesis and ligation steps. Rad1-Rad10-Slx4 is hypothesized to act in 3′ nonhomologous tail removal at this step. (B) Mating-type switching involving two nonhomologous ends due to insertion of *KANMX* sequence on the distal side of the break. A 3′ nonhomologous tail removal step is required to allow priming of DNA synthesis off of the invading strand. Repair then proceeds as above.

Mating-type switching was induced in *MAT***a** strains expressing HO endonuclease from the galactose-inducible *GAL10* promoter (MATERIALS AND METHODS). As shown in Table 2, cell viability following DSB induction was high in wild type (76% ± 3%) but reduced in *rad1*Δ (59% ± 2%; $P < 0.01$, Student's *t*-test) and *rad1*Δ *rad10*Δ double mutants (63% ± 1%; data not shown). The decrease in cell viability was specific to strains induced for *MAT***a** to *MAT*α switching; no significant decrease was observed in strains induced for completely homologous switching (*MAT***a** to *MAT***a**) that does not involve 3′ nonhomologous tails (Table 2). In addition, the percentage of surviving cells that had switched mating type was reduced in *rad1*Δ strains relative to wild type (71% ± 3% *vs.* 86% ± 3%; $P < 0.01$). This decrease in gene conversion may be due to an increase in repair of the break by nonhomologous end joining to yield *MAT***a** cells or could be indicative of aberrant repair or more disruptive nonhomologous end joining that disrupts the *MAT* locus and yields an "**a**-like faker" phenotype, since cells lacking a functional *MAT* locus phenocopy *MAT***a** by default (STRATHERN *et al.* 1981).

Recently, FLOTT *et al.* (2007) reported that the Slx4 protein forms a complex with Rad1-Rad10 and is critical for its 3′ nonhomologous tail removal activity during repair by SSA. As predicted from this work, Slx4 also functions with Rad1-Rad10 in mating-type switching. *slx4*Δ and *rad1*Δ *slx4*Δ mutants showed viability (57% ± 3% and 54% ± 2%, respectively) and switching phenotypes (68% ± 4% and 69% ± 4%, respectively) similar to *rad1*Δ strains (Table 2). In contrast, *msh2*Δ and *msh3*Δ strains displayed only a subtle decrease in viability (68%), and the percentage of switched cells was similar to wild type (Table 2). Thus, Msh2-Msh3 appears nearly dispensable for nonhomologous tail removal during mating-type switching, where the 3′ tail is on the non-invading strand.

We hypothesized that the gene conversion observed in the absence of Rad1-Rad10-Slx4 could be facilitated

TABLE 2

Viability and mating-type switching efficiency of wild-type and mutant strains

	% survival	% switched
One nonhomologous end (*MAT***a** to *MAT*α)		
Wild type	76.1 ± 3.1	85.7 ± 2.7
*rad1*Δ	58.6 ± 2.1*	70.6 ± 2.8*
*slx4*Δ	57.1 ± 2.5*	67.6 ± 3.9*
*rad1*Δ *slx4*Δ	54.4 ± 2.2*	69.3 ± 4.3*
*msh2*Δ	67.6 ± 4.0	80.6 ± 2.5
*msh3*Δ	67.9 ± 2.0	81.5 ± 3.0
*mus81*Δ	72.6 ± 1.7	88.7 ± 5.9
pol3-01	65.1 ± 5.1	83.2 ± 3.4
*rad1*Δ *mus81*Δ	56.1 ± 3.8*	74.5 ± 7.5
*rad1*Δ *pol3-01*	55.6 ± 5.2*	70.6 ± 3.8*
*rad9*Δ	75.1 ± 3.1	82.5 ± 2.6
*rad1*Δ *rad9*Δ	56.3 ± 2.7*	74.7 ± 3.3
Two homologous ends (*MAT***a** to *MAT***a**)		
Wild type	99.7 ± 2.2	NA
*rad1*Δ	95.3 ± 4.5	NA
*slx4*Δ	93.8 ± 4.3	NA
Two nonhomologous ends (*MAT***a**::*KANMX* to *MAT*α)		
Wild type	62.7 ± 3.7	72.8 ± 7.4
*rad1*Δ	26.8 ± 1.2*	0.8 ± 0.8*
*msh2*Δ	23.5 ± 2.9*	9.8 ± 2.3*
*msh3*Δ	29.9 ± 1.7*	10.0 ± 3.1*
*rad51*Δ	25.2 ± 2.7*	0.0 ± 0.0*

Percentage cell survival (induced/uninduced) was determined by examining the viability of cells plated after a 30-min induction of HO expression. Surviving cells were assayed to determine the percentage that had switched mating type from *MAT***a** to *MAT*α as described in MATERIALS AND METHODS. Data are presented as the mean ± SEM of at least four independent experiments. Asterisks indicate values significantly different from wild-type with $P < 0.01$, Students *t*-test. For one nonhomologous end (standard mating-type switching), nonhomologous sequence (**Ya**) is present on only the proximal side of the DSB. For two homologous ends, strains were induced for *MAT***a** to *MAT***a** switching; thus, "% switched" is not applicable (NA). For two nonhomologous ends, the indicated strains contain nonhomologous sequences on both sides of the DSB due to insertion of *KANMX* on the distal side of the break (see Figure 1B).

by the action of redundant nucleases that remove the 3′ **Ya** nonhomologous tail. However, disruption of Mus81-Mms4 or the polymerase δ 3′–5′ proofreading activity did not have a significant effect on the viability of *rad1*Δ mutants following mating-type switching (Table 2). Since mating-type switching can occur in *rad1*Δ mutants, albeit less efficiently, it is likely that unknown nucleases or multiple redundant nucleases are able to remove 3′ nonhomologous tails when Rad1-Rad10-Slx4 is absent. A recent study identified Saw1, a protein that interacts with Rad1-Rad10 and is thought to recruit Rad1-Rad10 to recombination intermediates (LI *et al.* 2008). It is possible that Saw1 may recruit other nucleases as well, allowing for completion of mating-type switching in the absence of Rad1-Rad10-Slx4.

Southern blot analysis was used to examine product formation in wild-type and *rad1*Δ strains during mating-type switching (Figure 2). Efficient DSB formation was observed at the *MAT* locus within 30 min of induction in all strains and products were detectable by 1 hr post-induction in wild type, consistent with previous studies (WHITE and HABER 1990; COLAIÁCOVO *et al.* 1999). *rad1*Δ mutants displayed a ~10% reduction in product formation relative to wild type. This result is much more subtle than that seen in an analysis of *MAT*α-to-*MAT***a** switching in G_1-arrested *rad1*Δ cells (HOLMES and HABER 1999b), but is consistent with the viability data presented above. The defects exhibited by mutants lacking Rad1-Rad10-Slx4 are more apparent in the pedigree, FACS, and chromatin immunoprecipitation studies described below and may indicate that, while *MAT*α product formation appears to be only mildly reduced in *rad1*Δ mutants, the gene conversion at *MAT* might be associated with BIR, aberrant recombination, or disrupted signaling.

Previous studies have shown a strict requirement for both Rad1-Rad10 and Msh2-Msh3 when both sides of a DSB contain nonhomologous sequence (SUGAWARA *et al.* 1997; COLAIÁCOVO *et al.* 1999). In repair of such breaks, a 3′ nonhomologous tail must be removed during the strand invasion step for repair DNA synthesis to proceed, in addition to 3′ nonhomologous removal at the later synthesis-dependent annealing step (Figure 1B). To confirm that Rad1-Rad10 and Msh2-Msh3 are required for removing 3′ nonhomologous tails on the invading strand during chromosomal mating-type switching, we inserted the *KANMX* sequence on the distal side of the HO cut site at the *MAT* locus (Figure 1B). In wild-type strains containing the *KANMX* insertion, gene conversion was delayed but completed with little loss of viability (Table 2; supplemental Figure 1). Consistent with previous studies, we found that both Rad1-Rad10 and Msh2-Msh3 complexes were required for gene conversion involving two 3′ nonhomologous tails. No gene conversion product was detected by Southern blot in *rad1*Δ and *msh3*Δ mutants (supplemental Figure 1), and the viability and switching efficiency of *rad1*Δ mutants was comparable to that of *rad51*Δ mutants completely defective in gene conversion, as shown in Table 2 (SUGAWARA *et al.* 1995). While the viability of *msh2*Δ and *msh3*Δ strains was equivalent to that of *rad1*Δ mutants, both *msh* mutants exhibited a greater percentage of switched cells (10%; Table 2), consistent with the idea that Msh2-Msh3 plays a supporting role that may be less critical than the role of Rad1-Rad10. The residual viability in *rad1*Δ, *msh2*Δ, *msh3*Δ, and *rad51*Δ strains is likely due to nonhomologous end joining, as seen in strains completely lacking donor sequences (MOORE and HABER 1996).

Prolonged Msh2 localization to the DSB in *rad1*Δ mutants: Because Rad1-Rad10 is predicted to remove 3′ nonhomologous tails on the non-invading strand fol-

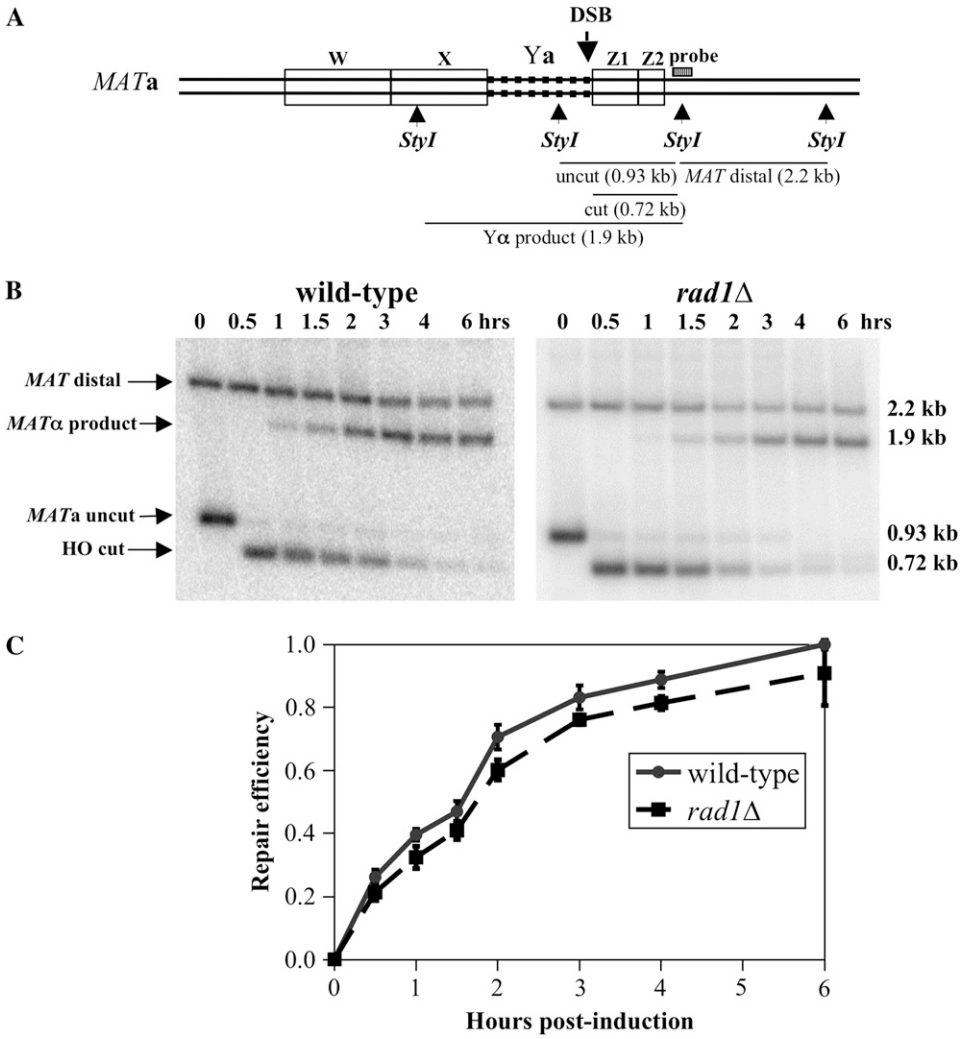

FIGURE 2.—Southern blot analysis of mating-type switching in wild-type and *rad1*Δ strains: (A) Diagram of the *MAT* locus showing the restriction sites used for Southern blot analysis, expected fragment lengths, and location of the probes used for detection of mating-type switching. (B) Analysis of digested DNA for wild-type and *rad1*Δ mutants induced for mating-type switching. Experiments were performed at least three times, with representative time courses shown. (C) Quantification of repair efficiency as described in MATERIALS AND METHODS.

lowing the annealing step (Figure 1), we reasoned that *rad1*Δ mutants would exhibit a delay in removal of the 3′ **Ya** sequence. Using **Ya**-specific probes, we were unable to detect a difference in the loss of **Ya** between wild-type and *rad1*Δ strains (supplemental Figure 2). Detection of any delay is confounded by the fact that the initial resection of the break should lead to loss of the 5′ strand of **Ya** with similar kinetics in both strains. Thus, we additionally performed chromatin immunoprecipitation using HA-tagged Msh2, α-HA antibody, and PCR primers located within the **Ya** sequence as described previously (GOLDFARB and ALANI 2004). Our lab previously showed that the Msh2 protein localizes rapidly to DSBs (EVANS *et al.* 2000).

As shown in Figure 3, Msh2 localized immediately to the *MAT* locus following DSB formation, peaked at 1 hr post-induction, and then decreased, consistent with the kinetics of product formation shown in Figure 2 and a role for Msh2-Msh3 in DSB repair. A similar pattern was seen using primers specific to the X-**Ya** junction; however, peak levels were achieved at a slightly later time point (1.5 hr; data not shown). While the input signal is lost over time due to conversion to *MAT*α, the input signal at the unrelated *CRY1* locus was constant throughout the time course.

In *rad1*Δ mutants, Msh2 localized to *MAT* following DSB formation, but in contrast to wild type, Msh2 remained near the break for ~3 hr (Figure 3). We observed a similar Msh2 localization pattern for *donorless* mutants unable to complete mating-type switching, where the 3′-ends are thought to be stable despite a complete inability to perform homologous repair (VAZE *et al.* 2002; AYLON *et al.* 2003). Msh2 localization was also prolonged at the X-**Ya** junction in *rad1*Δ compared to wild type (data not shown). Thus, while we were unable to detect a delay in loss of the **Ya** sequence in *rad1*Δ mutants, the prolonged presence of Msh2 at the break during mating-type switching suggests that at least a subset of *rad1*Δ mutants contain recombination intermediates at later time points.

***rad1*Δ mutants induced for mating-type switching exhibit G_2/M arrest:** The above observations encouraged us to examine the cell cycle progression of *rad1*Δ mutants during mating-type switching. Mutants lacking

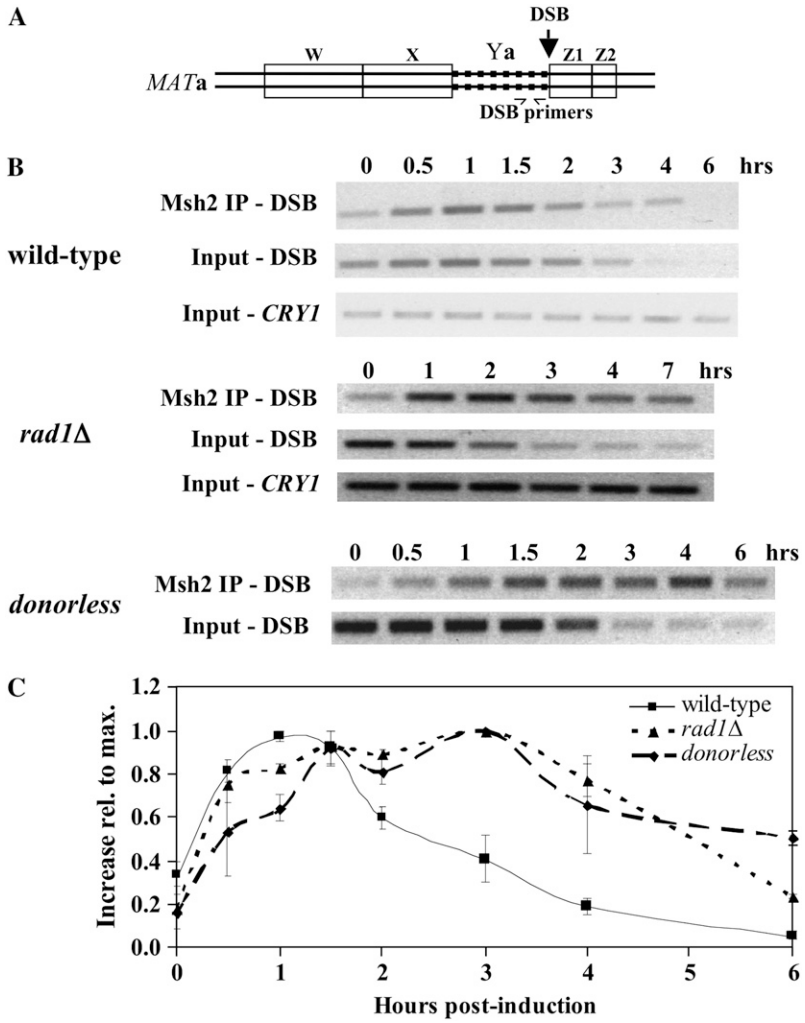

FIGURE 3.—Msh2 localization to the DSB in wild-type, *rad1*Δ, and *donorless* mutants. (A) Location of primers used for semiquantitative PCR following Msh2 chromatin immunoprecipitation. (B) Representative chromatin immunoprecipitation and PCR detection of Msh2 localization to *MAT* during mating-type switching in wild-type, *rad1*Δ, and *donorless* mutants. Since the **Ya** sequence is removed during mating-type switching, the input signal is also shown using primers to an unrelated locus (*CRY1*). (C) For each time point, the Msh2 ChIP signal was set relative to the $t = 0$ signal, with the maximum signal for each time course set as 1.0 to compare the relative the timing of Msh2 localization. Each data point represents the mean of three to four experiments ± SEM.

both donor sequences have previously been shown to exhibit a prolonged G_2/M cell cycle delay due to an inability to repair the DSB by homologous recombination (TOCZYSKI *et al.* 1997; LEE *et al.* 1998). We used FACS analysis to measure the DNA content of wild-type, *rad1*Δ, and *donorless* mutants following DSB induction. As shown in Figure 4, wild-type strains showed little variation in the percentage of cells in G_1, S, or G_2/M phase during the course of mating-type switching. Consistent with the known arrest phenotype, the majority of cells from a strain lacking both *HML*α and *HMR***a** sequences (*donorless*) were present in G_2/M phase at 4 hr (83.5% ± 1.5%) and 6 hr post-induction (71.8% ± 3.9%). *rad1*Δ strains showed a significant increase in the percentage of G_2/M cells at 2 hr (58.3% ± 4.0%) and 4 hr post-induction (65.1% ± 1.6%) relative to wild type (41.9% ± 1.5% and 30.1% ± 3.3%, respectively; $P < 0.01$), but returned to wild-type levels by 6 hr, suggesting that the absence of Rad1-Rad10 leads to a G_2/M arrest that is both shorter and earlier than observed in *donorless* mutants. This is consistent with gene conversion occurring in *rad1*Δ mutants, although inefficiently, in contrast to *donorless* mutants, which can survive only by nonhomologous end joining (MOORE and HABER 1996).

Mutants lacking Rad1-Rad10-Slx4 show unique viability profiles in pedigree analysis following mating-type switching: To further analyze the viability and cell cycle phenotypes seen in *rad1*Δ and *slx4*Δ mutants during mating-type switching, we performed pedigree experiments in which single, unbudded (G_1) cells were isolated after DSB formation and monitored through the cell cycle. Daughter cells were separated following the first cell division (MATERIALS AND METHODS). Cells that grew into colonies were subsequently assayed for mating type. As shown in Table 3, 96% of wild-type cells yielded two viable daughter cells that had both switched mating type. In contrast, only 38% of *rad1*Δ mutants formed two switched colonies and, of the remaining cells, 32% formed one switched colony and one dead cell cluster and 28% formed two dead cell clusters. *slx4*Δ and *rad1*Δ *slx4*Δ strains exhibited phenotypes similar to *rad1*Δ mutants (Table 3). No such decrease in viability was seen in these strains in the absence of the DSB, nor in *rad1*Δ strains induced for completely homologous *MAT***a** to *MAT***a** switching (Table 3B; data not shown).

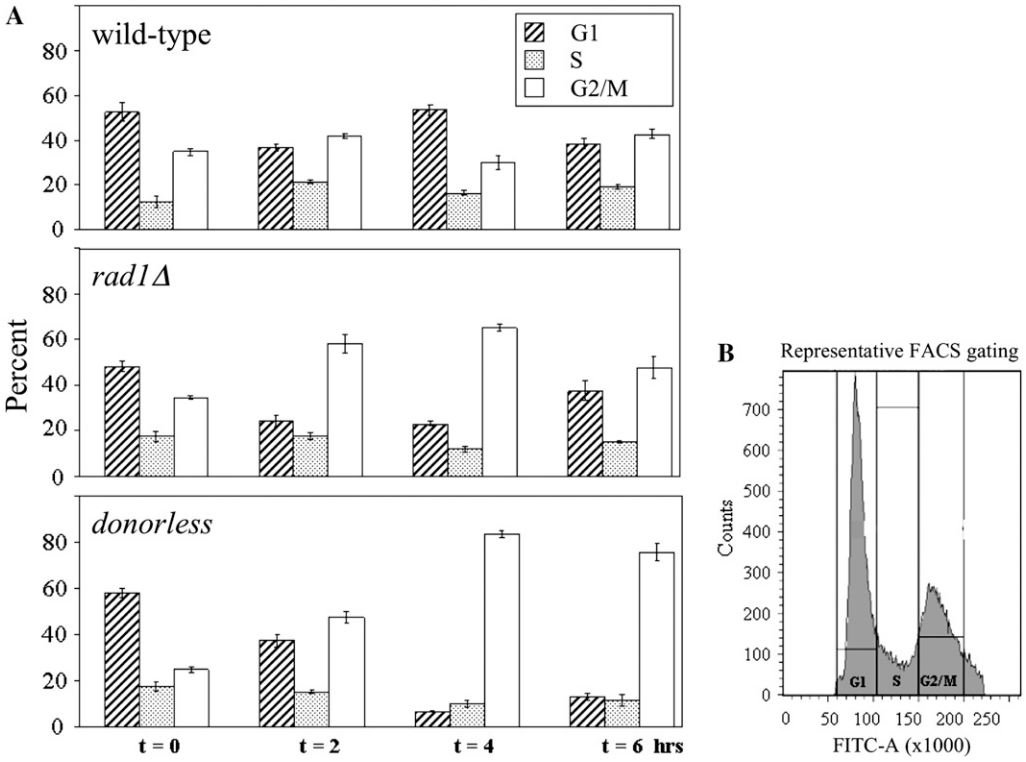

FIGURE 4.—FACS analysis of cells undergoing mating-type switching. (A) Bar graphs of the percentage of cells in G_1, S, or G_2/M phases of the cell cycle at 0, 2, 4, and 6 hr following induction of mating-type switching in wild-type, *rad1*Δ, and *donorless* strains (average of at least three experiments ± SEM). See MATERIALS AND METHODS for details. The increase in the percentage of G_2/M cells in *rad1*Δ mutants relative to wild type is statistically significant ($P < 0.01$ at $t = 2$ and $t = 4$ hr, Student's *t*-test). (B) Representative FACS profile for wild-type cells at $t = 0$, with vertical gates separating the $1n$ (G_1) and $2n$ (G_2/M) DNA content.

The "one switched, one dead" category is particularly intriguing, since repair and death arise from the same induced cell, and it is unique to cells undergoing gene conversion. Thus, the effect of the *rad1*Δ and *slx4*Δ mutations on mating-type switching is much more severe than was apparent in liquid culture assays, where asynchronous cells were induced for mating-type switching and the fate of daughter cells could not be assessed.

We also measured the length of the first cell division following DSB induction during the pedigree experiments. As shown in Table 4, completion of cell division was delayed by 3 hr in *rad1*Δ mutants compared to wild type ($P < 0.01$, Student's *t*-test), consistent with the FACS analysis presented above (Figure 4). Strains lacking donor sequences exhibited an even longer delay (10 ± 0.2 hr to complete division compared to 4.5 ± 0.1 hr in wild type; Table 4). During this extended period, *rad1*Δ and *donorless* cells displayed a large-budded morphology suggestive of G_2/M arrest (supplemental Figure 3A).

After completion of the first cell division, ~45% of *rad1*Δ cells failed to form colonies in the pedigree analysis (the dead cells from both the "two dead" and "one switched, one dead" categories), but divided several times before forming dead cell clusters (average of 8 ± 1 cells; supplemental Figure 3B). This phenotype is consistent with the phenomenon of break adaptation, in which cells exit the cell cycle arrest despite the continued presence of unrepaired DNA and differs from the death seen in cells undergoing DSB repair that fail to exit a G_2/M arrest (TOCZYSKI *et al.* 1997; LEE *et al.* 1998, 2003; PELLICIOLI *et al.* 2001). This adaptation phenotype is consistent with a significant proportion of *rad1*Δ cells induced for mating-type switching being unable to complete repair of the break. Inviable cells from *donorless* strains exhibited a more severe phenotype following checkpoint exit and died with one large-budded cell or two cells (adaptation for only one cycle) as documented previously (LEE *et al.* 1998), most likely due to the presence of more extensive DNA damage due to prolonged 5′–3′ resection.

Consistent with the cell survival assays described above, *msh2*Δ and *msh3*Δ mutations had little effect on viability during mating-type switching in pedigree experiments (Table 3, data not shown). Viability was reduced equally in both the induced and uninduced states, with ~80% of *msh2*Δ cells forming two viable colonies, ~10% forming one alive and one dead cell cluster, and ~10% with two inviable cells (Table 3). Thus the absence of *MSH2* confers a general decrease in viability that appears unrelated to the formation of an HO-induced DSB. A more subtle decrease in viability (5%) was observed for strains lacking *SLX4* in the uninduced state.

G_2/M delay in *rad1*Δ mutants is dependent upon both the DNA damage response and the spindle checkpoint: To test whether the cell division delay observed in *rad1*Δ mutants was mediated by the DNA damage checkpoint, we measured cell viability and cell cycle duration in *rad1*Δ mutants defective for the Rad9-dependent DNA damage response. *rad1*Δ *rad9*Δ double mutants exhibited cell cycle lengths comparable to wild-type and *rad9*Δ mutant cells (~5 hr; Table 4), in contrast to ~8 hr for *rad1*Δ mutants. Thus, the G_2/M cell cycle

TABLE 3

Pedigree analysis of wild type and mutants induced for mating-type switching (*MAT*a to *MAT*α) or mock induced

	% two switched	% one switched, one dead	% two dead	% other	*N*
		A. Induced			
Wild type	96	4	0	0	81
donorless	0	0	96	4	51
*rad1*Δ	38	32	28	2	97
*slx4*Δ	51	33	12	4	49
*rad1*Δ *slx4*Δ	29	44	19	8	59
*msh2*Δ	78	7	11	4	81
*rad9*Δ	82	12	6	0	90
*mad2*Δ	84	10	4	2	49
*rad1*Δ *rad9*Δ	20	41	39	0	102
*rad1*Δ *mad2*Δ	33	43	15	8	60
*mms2*Δ	79	7	12	2	58
*mph1*Δ	69	16	10	5	70
*rad1*Δ *mms2*Δ	19	54	26	1	99
*rad1*Δ *mph1*Δ	28	38	30	3	81
	% two alive	% one alive, one dead	% two dead		*N*
		B. Mock induced			
Wild type	99	0	1		91
donorless	100	0	0		41
*rad1*Δ	98	2	0		119
*slx4*Δ	94	3	3		36
*rad1*Δ *slx4*Δ	94	5	2		62
*msh2*Δ	84	9	7		76
*rad9*Δ	98	0	2		51
*mad2*Δ	100	0	0		26
*rad1*Δ *rad9*Δ	89	3	8		72
*rad1*Δ *mad2*Δ	91	2	8		53
*mms2*Δ	90	7	3		71
*mph1*Δ	100	0	0		52
*rad1*Δ *mms2*Δ	87	9	4		92
*rad1*Δ *mph1*Δ	96	3	1		75

Following induction of mating-type switching in liquid culture, single cells were separated on YPD medium under the light microscope using a microdissection needle. Cells were monitored at regular intervals, and daughter cells were separated after completion of the first cell division. Cells that formed colonies were tested for mating type as described in MATERIALS AND METHODS. The number of cells (*N*) tested for each strain is shown. For cells induced for mating-type switching, "% other" includes pairs of daughter cells scored as "one unswitched and one dead," or "one unswitched and one switched." Pairs of daughter cells scored as "both unswitched" were not included because we cannot rule out the failure to form a DSB in these cells. For the uninduced experiments, viability is shown for cells mock induced with water.

TABLE 4

Average length of cell cycle in cells undergoing mating-type switching

	Average time required for cell division (hr)			
	Uninduced	Two switched	One switched, one dead	Two dead
Wild type	4.5 ± 0.2	4.5 ± 0.1	NA	NA
donorless	4.9 ± 0.2	NA	NA	10 ± 0.2*
*rad1*Δ	4.7 ± 0.2	7.0 ± 0.3*	8.4 ± 0.3*	8.2 ± 0.4*
*slx4*Δ	4.7 ± 0.1	5.8 ± 0.2*	7.0 ± 0.4*	8.6 ± 0.4*
*rad1*Δ *slx4*Δ	4.5 ± 0.1	5.5 ± 0.4*	6.8 ± 0.4*	9.0 ± 0.4*
*msh2*Δ	4.3 ± 0.1	5.6 ± 0.1*	NA	6.5 ± 0.3*
*rad9*Δ	4.9 ± 0.1	4.5 ± 0.1	4.8 ± 0.2	NA
*mad2*Δ	4.9 ± 0.2	4.9 ± 0.2	4.2 ± 0.3	NA
*rad1*Δ *rad9*Δ	5.2 ± 0.1*	4.8 ± 0.2	4.8 ± 0.1	5.3 ± 0.1
*rad1*Δ *mad2*Δ	5.5 ± 0.2*	5.6 ± 0.3*	6.7 ± 0.3*	6.3 ± 0.2*
*mms2*Δ	4.5 ± 0.1	5.1 ± 0.1*	NA	6.1 ± 0.5*
*mph1*Δ	4.5 ± 0.1	4.7 ± 0.1	5.9 ± 0.6*	6.5 ± 0.8*
*rad1*Δ *mms2*Δ	4.5 ± 0.1	5.8 ± 0.3*	6.4 ± 0.1*	6.3 ± 0.1*
*rad1*Δ *mph1*Δ	5.3 ± 0.1*	6.2 ± 0.3*	8.1 ± 0.3*	8.3 ± 0.3*

Cell cycle duration was determined during pedigree analysis (see Table 3 and MATERIALS AND METHODS) and is shown as the mean length of time required for division (hr) ± SEM. "NA" denotes categories containing <10% of cells, and thus cell cycle lengths are not reported. Asterisks denote statistical significance from wild type with $P < 0.01$; values were compared to wild type "uninduced" or "two switched" as appropriate.

arrest exhibited by *rad1*Δ mutants is dependent upon *RAD9*, presumably via Rad9-mediated activation of the DNA damage response (HARRISON and HABER 2006). Elimination of the arrest had very little effect on the viability of *rad1*Δ mutants (Tables 2 and 3), pointing to an inability of the DNA damage response to promote repair.

Slx4 forms a complex with Rad1-Rad10 that is critical for 3′ nonhomologous tail removal during repair by single-strand annealing (FLOTT *et al.* 2007). As shown in Table 3, *slx4*Δ and *rad1*Δ *slx4*Δ mutants exhibited significantly shorter cell cycle delays than *rad1*Δ single mutants (1 *vs.* 2 hr for "two switched" and 2 *vs.* 3.5 hr for "one switched, one dead"). It is not surprising that the absence of Slx4 reduces the delay, since Slx4 is a known target of the Mec1 and Tel1 checkpoint kinases, requires checkpoint-dependent phosphorylation for Rad1-dependent SSA, and has been shown to regulate checkpoint-dependent processes (FLOTT and ROUSE 2005; ROBERTS *et al.* 2006; FLOTT *et al.* 2007). The fact that *slx4*Δ mutants exhibit *rad1*Δ-like phenotypes, but with shorter cell cycle delays, is additional evidence that Slx4 provides a link between the 3′-end-processing machinery and the DNA damage checkpoint.

Several studies have suggested a link between the DNA damage response and the spindle checkpoint (AYLON and KUPIEC 2003; KIM and BURKE 2008). We hypothesized that the cell death in *rad1*Δ mutants was due to aberrant repair involving gross chromosomal changes

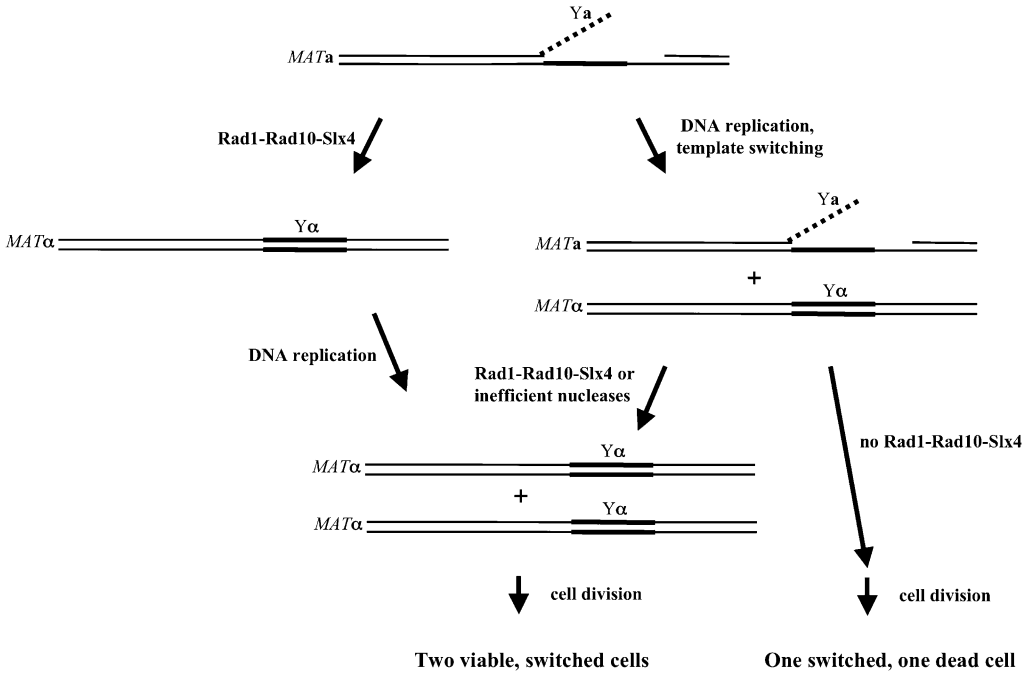

FIGURE 5.—Model for mating-type switching facilitated by DNA replication. We propose that mating-type switching can be mediated by ongoing DNA replication. DSB formation, 5′–3′ resection, strand invasion, synthesis, and repair of the invading strand occur as shown in Figure 1 and as predicted by SDSA models. The partially repaired recombination intermediate shown at the top containing a single-stranded break can then be acted on by either the DNA replication machinery or the Rad1-Rad10-Slx4 complex. In the presence of Rad1-Rad10-Slx4, the 3′ **Ya** nonhomologous tail is removed efficiently prior to, during, or following DNA replication, and once DNA replication has been completed, the cell can divide to produce two viable cells of the switched mating type. In the absence of Rad1-Rad10-Slx4, mating-type switching products are produced largely by replication of the partially repaired recombination intermediate to yield either one switched and one dead daughter cell or, after the action of inefficient nucleases, two viable switched daughters.

that might activate the spindle checkpoint and thus tested whether the G_2/M arrest in these mutants required *MAD2*. As shown in Tables 3 and 4, *mad2*Δ mutants induced for mating-type switching had only slightly decreased viability and displayed cell cycle lengths similar to wild type. However, *rad1*Δ *mad2*Δ double mutants exhibited reduced cell cycle delays relative to *rad1*Δ mutants (Table 4). Cells in the "two dead" and "one switched, one dead" pedigree categories took ~6.5 hr to divide in *rad1*Δ *mad2*Δ mutants, compared to ~8 hr in *rad1*Δ single mutants ($P < 0.015$). Interestingly, *rad1*Δ mutants that formed two switched colonies exhibited arrests that appeared fully *MAD2* dependent, unlike the partially *MAD2*-dependent arrests described above (Table 4). These results suggest that, although gene conversion occurs without loss of viability for cells in the "two switched" class, repair is inefficient and disruptive to the assembly of the mitotic spindle. The variety of arrest phenotypes in *rad1*Δ mutants further distinguishes the pedigree viability categories from each other and suggests that different defects or modes of repair operate in these subsets of cells.

Unique viability pattern in pedigree analysis is consistent with replication-mediated repair: Approximately one-third of *rad1*Δ mutant cells divided to form both one switched and one dead colony in the pedigree analysis (Table 3). We hypothesized that these cells may complete gene conversion by replicating partially repaired intermediates containing one intact switched strand and one unrepaired strand (Figure 5; KANG and SYMINGTON 2000). To test such a model, we examined whether post-replicative lesion bypass repair pathways were involved in completing gene conversion during mating-type switching. We focused on *MMS2*- and *MPH1*-dependent repair pathways, mutations in which cause defects in the error-free bypass pathways involving fork reversal and recombinational replication restart, respectively (TORRES-RAMOS *et al.* 2002; SCHÜRER *et al.* 2004; WATTS 2006). Both *mms2*Δ and *mph1*Δ mutants displayed decreased viability in the wild-type background during mating-type switching. As shown in Table 3, the percentage of cells in the "two switched" category for pedigree analysis was reduced to 79% in *mms2*Δ and 69% in *mph1*Δ mutants compared to 96% in wild type. *mms2*Δ mutants also displayed a slight reduction in viability in the absence of the DSB (Table 3), but viability was further decreased for cells induced for switching. Both of these mutants had an increased proportion of cells in both the "one switched, one dead" and "two dead" categories, indicating that replicative lesion bypass pathways play a role in the completion of gene conversion during mating-type switching.

To test whether the error-free lesion bypass pathways are responsible for repair in the absence of Rad1-Rad10-Slx4, we analyzed both *rad1*Δ *mms2*Δ and *rad1*Δ *mph1*Δ double mutants in pedigree experiments. *rad1*Δ *mms2*Δ double mutants exhibited a decrease in the percentage of "two switched" cells from 38 to 19%, and this decrease was directly correlated with an increase in the "one switched, one dead" category; however, no change in the percentage of "two dead" cells was seen for either *rad1*Δ *mms2*Δ or *rad1*Δ *mph1*Δ relative to *rad1*Δ single

mutants, suggesting that death of these cells occurs by a separate mechanism. The *mph1*Δ mutation appeared roughly epistatic to *rad1*Δ in this assay, with very little decrease in viability relative to *rad1*Δ.

The *mms2*Δ mutation reduced the length of cell cycle delay in *rad1*Δ mutants from 2 hr to 1 hr for the "two switched" cells and from 3.5 to 2 hr for the "one switched, one dead" and "two dead" categories (Table 4). *rad1*Δ *mph1*Δ double mutants exhibited a similar decrease in length of arrest for "two switched" cells, but not for dying cells. Thus, it is tempting to speculate that checkpoint signaling in *rad1*Δ mutants might be initiated or enhanced by the collision of a replication fork with recombination intermediates (see DISCUSSION). Together, the above phenotypes suggest a role for post-replicative lesion bypass repair in the completion of gene conversion during mating-type switching.

DISCUSSION

In this study, we investigated the requirements for the Rad1-Rad10, Slx4, and Msh2-Msh3 factors in 3′ nonhomologous tail removal during gene conversion at the chromosomal *MAT* locus. Rad1-Rad10 and Msh2-Msh3 have been proposed to act during mating-type switching in steps involving the removal of a single 3′ nonhomologous tail on the non-invading strand, primarily on the basis of their roles in 3′ nonhomologous tail removal during single-strand annealing and in plasmid-based assays (HABER 1998; PÂQUES and HABER 1999). As described above, mating-type switching in *rad1*Δ mutants led to a checkpoint-dependent G_2/M cell cycle delay and decreased viability. In the absence of functional Rad1-Rad10-Slx4, cells displayed a unique viability profile consistent with a model in which gene conversion can be facilitated by replication of partially repaired recombination intermediates. Msh2-Msh3, however, played only a subtle role in such repair, in contrast to its critical role in DSB repair involving two 3′ nonhomologous tails.

Previous work in the Symington lab proposed that replication of partially repaired recombination intermediates might bypass the requirement for Rad1-Rad10-dependent 3′ nonhomologous tail removal in a plasmid retention assay (KANG and SYMINGTON 2000). We extend this model to explain the unique viability pattern observed in *rad1*Δ and *slx4*Δ mutants in pedigree experiments, where one-third of cells divide to produce both repaired (switched) and dead daughter cells (Table 3, Figure 5). In this model, mutants lacking Rad1-Rad10-Slx4 initiate repair normally, but encounter difficulty after annealing of the repaired invading strand back to the *MAT* locus. In the absence of 3′ nonhomologous tail removal activity, the remaining broken strand is unable to prime repair DNA synthesis to complete gene conversion. If, instead, DNA replication occurs prior to 3′ nonhomologous tail removal, template switching could produce both an intact chromosome of the switched mating type and a broken chromosome. Segregation of these chromosomes to daughter cells could then lead to the "one switched, one dead" phenotype (Table 3), whereas repair of the broken chromosome by an inefficient nuclease could yield two viable, switched cells as seen in wild type (Figure 5). In further support of replication-mediated repair, another study found that mating-type switching in G_1-arrested cells led to a much more severe reduction in product formation (37% product formation at 5 hr) in *rad1*Δ mutants than is seen in this study in cycling cells, with product formation in *rad1*Δ mutants reduced to only ~90% of wild type at 4 hr (HOLMES and HABER 1999b). Additional evidence for this model of replication-mediated recombination is discussed below.

We show that mating-type switching in mutants lacking Rad1-Rad10 or Slx4 induces a G_2/M cell cycle delay involving both the DNA damage and spindle checkpoints (Table 4). Interestingly, the arrest phenotypes correlated with the viability phenotypes observed by pedigree analysis. Those cells that produced two viable, switched daughter cells exhibited shorter cell cycle delays (~2 hr) that were completely dependent upon the spindle checkpoint, whereas cells that produced two dead cell clusters or one switched colony and one dead cell cluster exhibited longer arrests (~3.5 hr) and were only partially dependent on the spindle checkpoint (Table 4).

Several studies have indicated potential links between the DNA damage and spindle checkpoints (GARBER and RINE 2002; KIM and BURKE 2008). It is not surprising that DNA damage that triggers the damage checkpoint might also impede the correct attachment and formation of tension between the chromosomes and the mitotic spindle. It was recently demonstrated that the spindle assembly checkpoint arrests cells in response to MMS-induced DNA damage in a Mec1- and Tel1-dependent manner, independent of a functional kinetochore (KIM and BURKE 2008). We show here that, in response to a single DSB at the *MAT* locus, the DNA damage response factor Rad9 appears to be required for both the DNA damage and spindle checkpoints, as *rad1*Δ *rad9*Δ mutants exhibit no G_2/M arrest and *rad1*Δ *mad2*Δ mutants exhibit shorter arrests than *rad1*Δ single mutants (1 *vs.* ~3.5 hr; Table 4). In contrast to other studies, we do not see residual G_2/M arrest in *rad9*Δ mutants in these experiments (AYLON and KUPIEC 2003; KIM and BURKE 2008).

Previous work has shown that the length of G_2/M arrest in response to DNA damage correlates with the amount of single-stranded DNA present (LEE *et al.* 1998). Our results are consistent with this, as *rad1*Δ mutants exhibit shorter arrests relative to *donorless* strains; *rad1*Δ mutants are able to initiate strand invasion, whereas *donorless* mutants accumulate ssDNA because they cannot initiate repair (LEE *et al.* 1998). We

also observed distinct adaptation phenotypes in the *rad1*Δ and *donorless* strains. *donorless* strains adapted for one cell cycle only and died at the next G_2/M transition, whereas *rad1*Δ mutants exhibited a classical break adaptation phenotype and died as eight-cell clusters (supplemental Figure 3). Since dying *rad1*Δ mutants exhibit a cell cycle delay followed by adaptation, it is possible that repair in this subset of the population occurs by BIR or by crossing over. BIR initiated from the *MAT* locus by strand invasion into *HML*α would lead to loss of half of chromosome *III*, including the centromere, and crossing over would similarly create an intrachromosomal deletion. Such repair would be expected to be associated with delayed product formation as well as with a DNA damage checkpoint- and spindle checkpoint-dependent G_2/M arrest, as seen in our pedigree analysis (McEachern and Haber 2006).

The fact that Msh2 localization to the *MAT* locus is prolonged in *rad1*Δ and *donorless* mutants implies the presence of unrepaired recombination intermediates several hours after DSB formation. While this is expected in *donorless* mutants that lack homologous donor sequences, the fact that *rad1*Δ mutants exhibit *donorless*-like Msh2 localization highlights the fact that repair occurs aberrantly in these cells. The prolonged presence of Msh2 in both mutants is also consistent with the fact that these mutants have an activated DNA damage response and may indicate a role for Msh2 in this checkpoint.

In contrast to proposed models of mating-type switching and to gene conversion involving a 3′ nonhomologous tail on the invading strand, Rad1-Rad10-dependent 3′ nonhomologous tail removal on the second, noninvading strand appears to be independent of Msh2-Msh3. Viability was only slightly reduced in *msh2*Δ mutants undergoing mating-type switching, and *msh2*Δ mutants did not exhibit the unique viability pattern characteristic of *rad1*Δ and *slx4*Δ mutants in pedigree analysis. In this way, Rad1-Rad10-dependent 3′ nonhomologous tail removal during mating-type switching is analogous to its role in cleavage of 3′ DNA-bound Top1 lesions, which is also Msh2-Msh3 independent (Vance and Wilson 2002).

There are at least two separate error-free lesion bypass pathways in *S. cerevisiae*: one pathway involves the homologous recombination machinery and the Mph1 helicase and the second pathway is the Rad5-Mms2-Ubc13 branch of the Rad6-Rad18 pathway that is thought to regress replication forks and promote bypass of lesions by template switching (Torres-Ramos *et al.* 2002; Schürer *et al.* 2004; Watts 2006; Blastyák *et al.* 2007). We observed that both of these pathways contributed to the viability and cell cycle phenotypes of cells undergoing mating-type switching. Mph1 is a helicase that is known to be in the Rad52 epistasis group, but it is thought to function in recombinational restart of stalled replication forks (Schürer *et al.* 2004; Prakash *et al.* 2005). The fact that the *rad1*Δ and *mph1*Δ mutations were mostly epistatic suggests that the Mph1-dependent fork restart is hindered by the presence of the nonhomologous 3′-end that remains in *rad1*Δ mutants, although it is unclear why this might be. We cannot rule out that the role of the Mph1 helicase during gene conversion is separate from its role in replication fork restart.

Replicative lesion bypass pathway choice depends on whether the lesion (in this case, a 3′ nonhomologous tail followed by a significant single-stranded gap) is on the leading strand *vs.* on the lagging strand. Presumably, priming of the next Okazaki fragment on the lagging strand could bypass such a lesion and allow replication to proceed without employing specialized fork restart machinery, which may explain why the decreased viability in *mms2*Δ and *mph1*Δ mutants is relatively subtle. In addition, there is *in vitro* evidence using bacterial proteins that repriming of DNA synthesis can occur on the leading strand (Heller and Marians 2006). The nearest replication origin to the *MAT* locus is located on the centromere-proximal side, ~2.5 kb from the Y region at *MAT* (http://www.oridb.org; http://www.yeastgenome.org), so it may be more likely that the 3′ **Ya** tail is replicated by lagging- rather than leading-strand synthesis.

Mating-type switching does not require progression through S-phase, since efficient gene conversion is detected in G_2-arrested cells, although *MAT* switching in G_1-arrested cells is severely reduced due to the absence of CDK1 (Cdc28) activation (Holmes and Haber 1999b; Ira *et al.* 2004; Wang *et al.* 2004). However, DNA replication may contribute to mating-type switching by priming DNA synthesis across the top strand of the partially repaired intermediate pictured in Figure 5, bypassing the need to use the cleaved 3′-end as a primer for repair synthesis and relaxing the dependence on Rad1-Rad10-Slx4. Indeed, mutations in the genes encoding polymerase α-primase or Rad27 were shown to greatly reduce mating-type switching in G_1-arrested cells (Holmes and Haber 1999b). While it was later shown that these lagging-strand synthesis factors were dispensable for mating-type switching in G_2-arrested cells (Wang *et al.* 2004), it is possible that cycling cells might utilize lagging-strand synthesis in addition to specialized lesion bypass pathways to promote efficient completion of gene conversion. Moreover, recent work has shown that endonuclease-induced DSBs formed during G_1 are recognized by the RPA subunit Rfa1 only after cells have entered S-phase and that formation of Rad52 foci following irradiation treatment required release of G_1-arrested cells into S-phase (Barlow *et al.* 2008). Further studies will be necessary to parse out the interplay between DNA replication and repair of DSBs by homologous recombination.

In summary, we conclude that gene conversion intermediates containing 3′ nonhomologous tails are principally processed by Rad1-Rad10-Slx4, even on the

non-invading strand, and we propose that repair is aided by concurrent DNA replication and its associated post-replicative lesion bypass pathways.

We thank James Haber and Neal Sugawara for strains, plasmids, advice, and comments on the manuscript; Lorraine Symington and John Rouse for insights regarding the *rad1*Δ and *slx4*Δ mutant phenotypes; Aaron Plys for construction of *mms2*Δ and *pol3-01* strains; and members of the Alani lab for comments on the manuscript. A.M.L. was supported by a Graduate Assistance in Areas of National Need fellowship from the U. S. Department of Education and a National Institutes of Health (NIH) Training Grant, T.G. by a Natural Sciences and Engineering Research Council of Canada Post Graduate Scholarship B Award, and E.A. by NIH grant GM53085.

LITERATURE CITED

Aylon, Y., and M. Kupiec, 2003 The checkpoint protein Rad24 of *Saccharomyces cerevisiae* is involved in processing double-strand break ends and in recombination partner choice. Mol. Cell. Biol. **23:** 6585–6596.

Aylon, Y., B. Liefshitz, G. Bitan-Banin and M. Kupiec, 2003 Molecular dissection of mitotic recombination in the yeast *Saccharomyces cerevisiae*. Mol. Cell. Biol. **23:** 1403–1417.

Bardwell, A., L. Bardwell, A. Tomkinson and E. Friedberg, 1994 Specific cleavage of model recombination and repair intermediates by the yeast Rad1-Rad10 DNA endonuclease. Science **265:** 2082–2085.

Barlow, J. H., M. Lisby and R. Rothstein, 2008 Differential regulation of the cellular response to DNA double-strand breaks in G1. Mol. Cell **30:** 73–85.

Blastyák, A., L. Pintér, I. Unk, L. Prakash, S. Prakash *et al.*, 2007 Yeast Rad5 protein required for postreplication repair has a DNA helicase activity specific for replication fork regression. Mol. Cell **28:** 167–175.

Church, G. M., and W. Gilbert, 1984 Genomic sequencing. Proc. Natl. Acad. Sci. USA **81:** 1991–1995.

Colaiácovo, M. P., F. Pâques and J. E. Haber, 1999 Removal of one nonhomologous DNA end during gene conversion by a *RAD1*- and *MSH2*-independent pathway. Genetics **151:** 1409–1423.

Evans, E., N. Sugawara, J. E. Haber and E. Alani, 2000 The *Saccharomyces cerevisiae* Msh2 mismatch repair protein localizes to recombination intermediates *in vivo*. Mol. Cell **5:** 189–199.

Fishman-Lobell, J., and J. Haber, 1992 Removal of nonhomologous DNA ends in double-strand break recombination: the role of the yeast ultraviolet repair gene *RAD1*. Science **258:** 480–484.

Flott, S., and J. Rouse, 2005 Slx4 becomes phosphorylated after DNA damage in a Mec1/Tel1-dependent manner and is required for repair of DNA alkylation damage. Biochem. J. **391:** 325–333.

Flott, S., C. Alabert, G. W. Toh, R. Toth, N. Sugawara *et al.*, 2007 Phosphorylation of Slx4 by Mec1 and Tel1 regulates the single-strand annealing mode of DNA repair in budding yeast. Mol. Cell. Biol. **27:** 6433–6445.

Garber, P. M., and J. Rine, 2002 Overlapping roles of the spindle assembly and DNA damage checkpoints in the cell-cycle response to altered chromosomes in *Saccharomyces cerevisiae*. Genetics **161:** 521–534.

Gietz, R. D., and R. H. Schiestl, 1991 Applications of high efficiency lithium acetate transformation of intact yeast cells using single-stranded nucleic acids as carrier. Yeast **7:** 253–263.

Goldfarb, T., and E. Alani, 2004 Chromatin immunoprecipitation to investigate protein-DNA interactions during genetic recombination, pp. 223–237 in *Genetic Recombination: Reviews and Protocols*, edited by A. S. Waldman. Humana Press, Totowa, NJ.

Goldfarb, T., and E. Alani, 2005 Distinct roles for the *Saccharomyces cerevisiae* mismatch repair proteins in heteroduplex rejection, mismatch repair and nonhomologous tail removal. Genetics **169:** 563–574.

Guzder, S. N., C. Torres-Ramos, R. E. Johnson, L. Haracska, L. Prakash *et al.*, 2004 Requirement of yeast Rad1-Rad10 nuclease for the removal of 3′-blocked termini from DNA strand breaks induced by reactive oxygen species. Genes Dev. **18:** 2283–2291.

Haber, J. E., 1998 Mating-type gene switching in *Saccharomyces cerevisiae*. Annu. Rev. Genet. **32:** 561–599.

Harrison, J. C., and J. E. Haber, 2006 Surviving the breakup: the DNA damage checkpoint. Annu. Rev. Genet. **40:** 209–235.

Heller, R. C., and K. J. Marians, 2006 Replication fork reactivation downstream of a blocked nascent leading strand. Nature **439:** 557–562.

Holmes, A., and J. E. Haber, 1999a Physical monitoring of HO-induced homologous recombination. Methods Mol. Biol. **113:** 403–415.

Holmes, A. M., and J. E. Haber, 1999b Double-strand break repair in yeast requires both leading and lagging strand DNA polymerases. Cell **96:** 415–424.

Ira, G., A. Pellicioli, A. Balijja, X. Wang, S. Fiorani *et al.*, 2004 DNA end resection, homologous recombination and DNA damage checkpoint activation require CDK1. Nature **431:** 1011–1017.

Ira, G., D. Satory and J. E. Haber, 2006 Conservative inheritance of newly synthesized DNA in double-strand break-induced gene conversion. Mol. Cell. Biol. **26:** 9424–9429.

Ivanov, E., and J. Haber, 1995 *RAD1* and *RAD10*, but not other excision repair genes, are required for double-strand break-induced recombination in *Saccharomyces cerevisiae*. Mol. Cell. Biol. **15:** 2245–2251.

Kang, L. E., and L. S. Symington, 2000 Aberrant double-strand break repair in *rad51* mutants of *Saccharomyces cerevisiae*. Mol. Cell. Biol. **20:** 9162–9172.

Kim, E. M., and D. J. Burke, 2008 DNA damage activates the SAC in an ATM/ATR-dependent manner, independently of the kinetochore. PLoS Genet. **4:** e1000015.

Kirkpatrick, D. T., and T. D. Petes, 1997 Repair of DNA loops involves DNA-mismatch and nucleotide-excision repair proteins. Nature **387:** 929–931.

Klar, A. J. S., and J. N. Strathern, 1984 Resolution of recombination intermediates generated during yeast mating type switching. Nature **310:** 744–748.

Lee, S. E., J. K. Moore, A. Holmes, K. Umezu, R. D. Kolodner *et al.*, 1998 *Saccharomyces* Ku70, Mre11/Rad50, and RPA proteins regulate adaptation to G2/M arrest after DNA damage. Cell **94:** 399–409.

Lee, S. E., A. Pellicioli, M. B. Vaze, N. Sugawara, A. Malkova *et al.*, 2003 Yeast Rad52 and Rad51 recombination proteins define a second pathway of DNA damage assessment in response to a single double-strand break. Mol. Cell. Biol. **23:** 8913–8923.

Li, F., J. Dong, X. Pan, J.-H. Oum, J. D. Boeke *et al.*, 2008 Microarray-based genetic screen defines *SAW1*, a gene required for Rad1/Rad10-dependent processing of recombination intermediates. Mol. Cell **30:** 325–335.

McEachern, M. J., and J. E. Haber, 2006 Break-induced replication and recombinational telomere elongation in yeast. Annu. Rev. Biochem. **75:** 111–135.

McGill, C., B. Shafer and J. Strathern, 1989 Coconversion of flanking sequences with homothallic switching. Cell **57:** 459–467.

McWhir, J., J. Selfridge, D. J. Harrison, S. Squires and D. W. Melton, 1993 Mice with DNA repair gene (*ERCC-1*) deficiency have elevated levels of p53, liver nuclear abnormalities and die before weaning. Nat. Genet. **5:** 217–224.

Moore, J., and J. Haber, 1996 Cell cycle and genetic requirements of two pathways of nonhomologous end-joining repair of double-strand breaks in *Saccharomyces cerevisiae*. Mol. Cell. Biol. **16:** 2164–2173.

Pâques, F., and J. E. Haber, 1997 Two pathways for removal of nonhomologous DNA ends during double-strand break repair in *Saccharomyces cerevisiae*. Mol. Cell. Biol. **17:** 6765–6771.

Pâques, F., and J. E. Haber, 1999 Multiple pathways of recombination induced by double-strand breaks in *Saccharomyces cerevisiae*. Microbiol. Mol. Biol. Rev. **63:** 349–404.

Pellicioli, A., C. Lucca, G. Liberi, F. Marini, M. Lopes *et al.*, 1999 Activation of Rad53 kinase in response to DNA damage and its effect in modulating phosphorylation of the lagging strand DNA polymerase. EMBO J. **18:** 6561–6572.

Pellicioli, A., S. E. Lee, C. Lucca, M. Foiani and J. E. Haber, 2001 Regulation of *Saccharomyces* Rad53 checkpoint kinase during adaptation from DNA damage-induced G2/M arrest. Mol. Cell **7:** 293–300.

Prakash, R., L. Krejci, S. Van Komen, K. Anke Schürer, W. Kramer *et al.*, 2005 Saccharomyces cerevisiae *MPH1* gene, required for

homologous recombination-mediated mutation avoidance, encodes a 3′ to 5′ DNA helicase. J. Biol. Chem. **280:** 7854–7860.

Roberts, T. M., M. S. Kobor, S. A. Bastin-Shanower, M. Ii, S. A. Horte *et al.*, 2006 Slx4 regulates DNA damage checkpoint-dependent phosphorylation of the BRCT domain protein Rtt107/Esc4. Mol. Biol. Cell **17:** 539–548.

Rose, M. D., F. Winston and P. Hieter, 1990 *Methods in Yeast Genetics*. Cold Spring Harbor Laboratory Press, Cold Spring Harbor, NY.

Sandell, L. L., and V. A. Zakian, 1993 Loss of yeast telomere: arrest, recovery, and chromosome loss. Cell **75:** 729–739.

Saparbaev, M., L. Prakash and S. Prakash, 1996 Requirement of mismatch repair genes *MSH2* and *MSH3* in the *RAD1-RAD10* pathway of mitotic recombination in *Saccharomyces cerevisiae*. Genetics **142:** 727–736.

Schürer, K. A., C. Rudolph, H. D. Ulrich and W. Kramer, 2004 Yeast *MPH1* gene functions in an error-free DNA damage bypass pathway that requires genes from homologous recombination, but not from postreplicative repair. Genetics **166:** 1673–1686.

Strathern, J., J. Hicks and I. Herskowitz, 1981 Control of cell type in yeast by the mating type locus. J. Mol. Biol. **147:** 357–372.

Sugawara, N., E. L. Ivanov, J. Fishman-Lobell, B. L. Ray, X. Wu *et al.*, 1995 DNA structure-dependent requirements for yeast *RAD* genes in gene conversion. Nature **373:** 84–86.

Sugawara, N., F. Pâques, M. Colaiacovo and J. E. Haber, 1997 Role of *Saccharomyces cerevisiae* Msh2 and Msh3 repair proteins in double-strand break-induced recombination. Proc. Natl. Acad. Sci. USA **94:** 9214–9219.

Sung, P., P. Reynolds, L. Prakash and S. Prakash, 1993 Purification and characterization of the *Saccharomyces cerevisiae* RAD1/RAD10 endonuclease. J. Biol. Chem. **268:** 26391–26399.

Surtees, J. A., and E. Alani, 2006 Mismatch repair factor MSH2-MSH3 binds and alters the conformation of branched DNA structures predicted to form during genetic recombination. J. Mol. Biol. **360:** 523–526.

Toczyski, D. P., D. J. Galgoczy and L. H. Hartwell, 1997 *CDC5* and CKII control adaptation to the yeast DNA damage checkpoint. Cell **90:** 1097–1106.

Torres-Ramos, C. A., S. Prakash and L. Prakash, 2002 Requirement of *RAD5* and *MMS2* for postreplication repair of UV-damaged DNA in *Saccharomyces cerevisiae*. Mol. Cell. Biol. **22:** 2419–2426.

Vance, J. R., and T. E. Wilson, 2002 Yeast Tdp1 and Rad1-Rad10 function as redundant pathways for repairing Top1 replicative damage. Proc. Natl. Acad. Sci. USA **99:** 13669–13674.

Vaze, M. B., A. Pellicioli, S. E. Lee, G. Ira, G. Liberi *et al.*, 2002 Recovery from checkpoint-mediated arrest after repair of a double-strand break requires Srs2 helicase. Mol. Cell **10:** 373–385.

Wach, A., A. Brachat, R. Pöhlmann and P. Philippsen, 1994 New heterologous modules for classical or PCR-based gene disruptions in *Saccharomyces cerevisiae*. Yeast **10:** 1793–1808.

Wang, X., G. Ira, J. A. Tercero, A. M. Holmes, J. F. X. Diffley *et al.*, 2004 Role of DNA replication proteins in double-strand break-induced recombination in *Saccharomyces cerevisiae*. Mol. Cell. Biol. **24:** 6891–6899.

Watts, F. Z., 2006 Sumoylation of PCNA: wrestling with recombination at stalled replication forks. DNA Repair **5:** 399–403.

Weeda, G., I. Donker, J. De Wit, H. Morreau, R. Janssens *et al.*, 1997 Disruption of mouse *ERCC1* results in a novel repair syndrome with growth failure, nuclear abnormalities and senescence. Curr. Biol. **7:** 427–439.

White, C. I., and J. E. Haber, 1990 Intermediates of recombination during mating type switching in *Saccharomyces cerevisiae*. EMBO J. **9:** 663–673.

Wu, X., and J. Haber, 1995 *MAT***a** donor preference in yeast mating-type switching: activation of a large chromosomal region for recombination. Genes Dev. **9:** 1922–1932.

Wu, X., and J. E. Haber, 1996 A 700 bp *cis*-acting region controls mating-type dependent recombination along the entire left arm of yeast chromosome III. Cell **87:** 277–285.

Wu, X., C. Wu and J. E. Haber, 1997 Rules of donor preference in Saccharomyces mating-type gene switching revealed by a competition assay involving two types of recombination. Genetics **147:** 399–407.

Communicating editor: P. Russell